

Molecular Dynamics Simulation of Adhesion Processes

Sung-San Cho*, Seungho Park

Department of Mechanical and System Design Engineering, Hongik University,
Seoul 121-791, Korea

Adhesion of a hemispherical tip to the flat surface in nano-structures is simulated using the molecular dynamics technique. The tip and plates are modeled with the Lennard-Jones molecules. The simulation focuses on the deformation of the tip. Detailed descriptions on the evolution of interaction force, the energy dissipation due to adhesion hysteresis, the formation-growth-breakage of adhesive junction as well as the evolution of molecular distribution during the process are presented. The effects of the tip size, the maximum tip approach, the tip temperature, and the affinity between the tip and the mating plate are also discussed.

Key Words : Molecular Dynamics Simulation, Adhesion, Nano-Structure

Nomenclature

D : Distance between upper and lower surfaces
 F : Force
 L : Simulation domain size
 m : Molecular mass
 N : Total number of molecules
 r_{ij} : Inter-distance between molecules i and j
 r_c : Cutoff radius
 R : Radius
 t : Time
 T : Temperature

Greek Symbols

α : Affinity factor
 ε : Energy parameter
 σ : Length parameter
 Φ : Potential function

Superscript

* : Dimensionless

Subscripts

i, j : i_{th} and j_{th} molecules
 p : Period for adhesion process

tip : For tip
 $upper$: For upper plate
 x, y, z : Directions in rectangular coordinate

1. Introduction

It is well known that adhesion is associated with friction. According to the adhesion theory of macroscopic friction (Rabinowicz, 1965), adhesively-bonded contacting asperities, so called junctions, form, grow and break while a tangential motion occurs between two contacting surfaces. The friction force is assumed to be the sum of the junction-breaking forces that can be estimated with two major parameters, i.e., the junction size and the junction-breaking shear stress. The junction size can be estimated with the well-developed adhesive contact models such as the JKR model (Johnson et al., 1971), DMT model (Derjaguin et al., 1975) or the finite element adhesive contact model (Cho and Park, 2002). Meanwhile, the nature of junction-breaking stress is not clearly identified yet, and the stress has been defined differently in the literatures (St-caffelini, 2001). Thus the origin of adhesion has been a major concern in the research of this field.

One of efficient computational methods in nano-scales is the molecular dynamics (MD)

* Corresponding Author,
E-mail : sscho@wow.hongik.ac.kr
TEL : +82-2-320-1674; FAX : +82-2-320-7003
Department of Mechanical and System Design Engineering, Hongik University Seoul 121-791, Korea.
(Manuscript Received May 7, 2002; Revised August 9, 2002)

simulation, which has long been used and well developed as tool in statistical mechanics and chemistry. This method has recently been employed to investigate the various nano-scale phenomena including tribological ones such as indentation and friction (Landman, 1998; Komanduri, et al., Richter et al., 2000; Christopher, et al., 2001; Zhang and Tanaka, 1997; 1998; Rafii-Tabar, 2000; Weng et al., 2000, Park, at al., 2002). These atomistic studies have revealed several new findings and helped improving our understanding these phenomena in nano-scales. Especially, several atomistic studies on friction have been reported. In these studies (Rafii-Tabar, 2000; Weng et al., 2000, Park, at al., 2002) primarily the friction mechanisms associated with plastic deformation such as plowing and cutting were investigated while the transfer of asperity molecules to the contacting surface and/or the deformation of the contacting asperity were restricted.

In this article, the adhesion process of a round-tip on a flat plate has been simulated using the molecular dynamics technique. The simulation focuses especially on the deformation of tip that has been rarely studied. The evolution of interaction force, the energy dissipation due to hysteresis, and the formation-growth-breakage of the junction as well as the evolution of molecular distribution in the process are investigated in detail. The Lennard-Jones molecules are applied to simplify the simulation. Although the Lennard-Jones potential simulates only the interactions between inert molecules such as Ar, Kr, Xe, it has been widely applied to understand various physical and thermal phenomena in nanoscale (Haile, 1992; Allen and Tildesley, 1987).

2. Molecular Dynamics Simulation

Investigation of the characteristics of adhesion process utilizes the Lennard-Jones (LJ) 12-6 potential, given as

$$\Phi(r_{ij}) = 4\epsilon \left[\left(\frac{\sigma}{r_{ij}} \right)^{12} - \left(\frac{\sigma}{r_{ij}} \right)^6 \right] \quad (1)$$

where the length parameter $\sigma = 0.34$ nm and the

energy parameter $\epsilon = 1.67 \times 10^{-21}$ J. These parameters are based on argon whose molecular mass is $m = 6.63 \times 10^{-26}$ kg. The r_{ij} denotes inter-distances between molecules i and j . This LJ potential is truncated to zero for distances larger than 2.5σ without long-range force corrections, which was widely applied to expedite the simulation (Allen and Tildesley, 1987). The molecular motion is simulated by solving Newton's equation of motion with intermolecular forces obtained from Eq. (1),

$$F_i = - \sum_{j \neq i}^n \frac{\partial \Phi(r_{ij})}{\partial r_i} = m_i \frac{d^2 r_i}{dt^2} \quad (2)$$

using the "velocity Verlet" algorithm (Swope et al., 1982) with a time-step of 5 fs or $\Delta t^* = 2.335 \times 10^{-3}$. In this work all quantities with an asterisk are nondimensionalized with respect to σ , ϵ , and m .

Before simulating an adhesion process, a crystalline fcc structure is designed and placed at the center of the computational domain for each simulation condition. Initial velocities of molecules are either estimated using the Maxwell-Boltzmann distribution at a given temperature or obtained from previous simulations, if available. This pre-designed molecular system undergoes an equilibration process of 100000 time-steps at temperature $T^* = 0.248$.

For simplification of the analysis, molecules constructing the upper and lower plates are assumed to be rigid at a fixed temperature ($T^* = 0.248$), while molecules in the hemispherical tip are allowed to move in accordance with Eq. (2). Since the tip is modelled as a hemisphere of radius $R_{tip}^* = 9.37$ and the distance between the upper and lower plates D^* is set equal to 11.72 in the initial configuration, the initial distance between the tip-end and the lower plate is 2.35. Since the cutoff radius r_c^* is 2.5, only the molecules in the tip-end region have a weak interaction with the lower surface at the beginning of the simulation. At time-step 10000 the upper plate starts to move down toward the lower plate and then recedes to the initial position, which can be modelled as

$$\Delta z_{upper}^*(t^*) = z_{upper}^*(t^*) - z_{upper}^*(0) = -A^*[1 - \cos(2\pi t^*/t_p^*)] \quad (3)$$

where half the maximum displacement A^* is 2.5 and the period of the tip movement t_p^* is 100000 time-steps. Each plate and the tip consist of 2048 and 1682 molecules, respectively. Although periodic boundary conditions are applied in the x and y directions (refer to Fig. 1), the interaction between the imaginary structure due to the periodicity and the tip in the simulation domain becomes negligible, since the calculation domain size is $L_x^* \times L_y^* = 25 \times 25$.

3. Results and Discussion

Figure 1 shows the snapshots of molecular distributions and normal forces experienced by the molecules in the top-most layer of the lower plate during an adhesion process. For the upper

plate movement $\Delta z_{upper}^* = -0.477$, the change in tip shape is hardly identified although the tip is attracted by the lower plate, as evidenced by the distribution of normal force. As the tip approaches the lower plate, the attraction becomes significant and affects a relatively larger area, as shown in the force distribution at $\Delta z_{upper}^* = -1.73$. As the pressing process goes further, the tip starts to contact the lower plate, interacting repulsively with the lower plate that can be seen in the force distribution at $\Delta z_{upper}^* = -2.5$. For the final stage of tip approach $\Delta z_{upper}^* = -5$ the shape of the tip has been changed significantly and appears to be an adhesive junction, in which the repulsive interaction is very significant. As the receding process starts, the repulsive interactions turn into attractive ones immediately, and then do not change considerably until the end of the receding process as shown in the force distri-

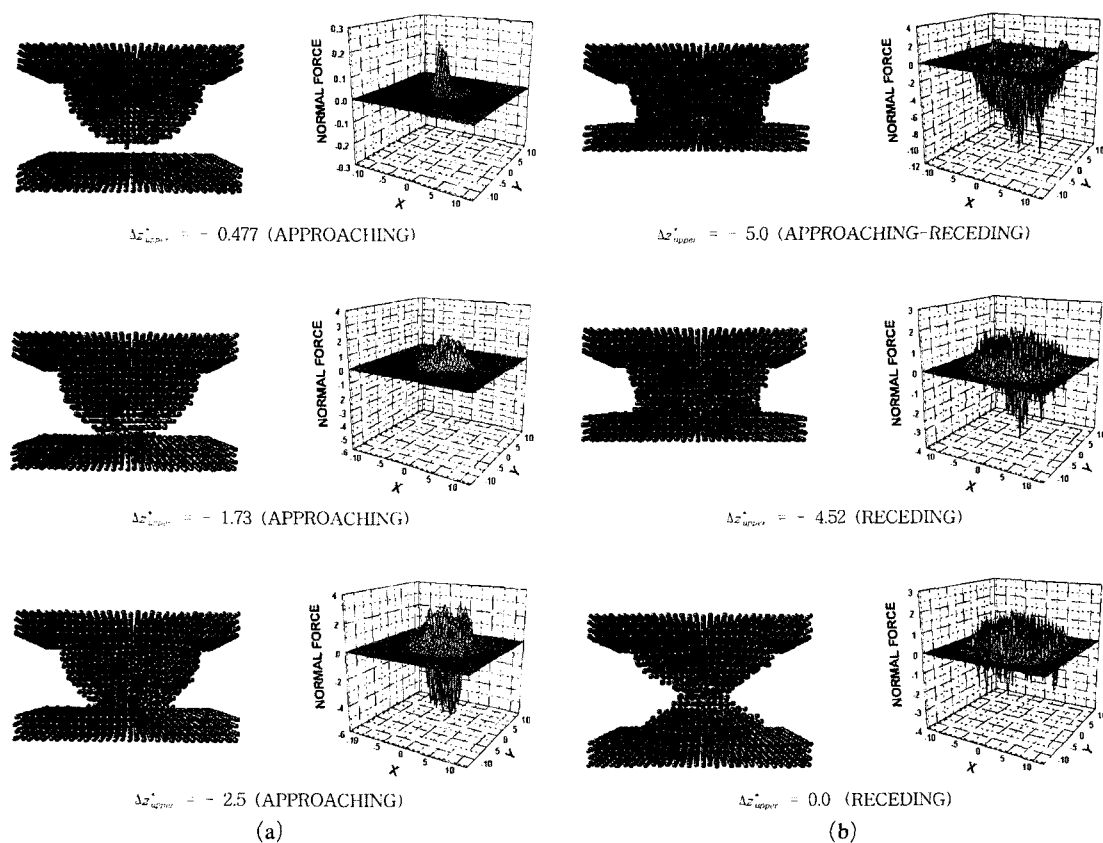


Fig. 1 Snapshots of molecular distribution and normal forces during adhesion processes

butions at $\Delta z_{upper}^* = -4.52$ and $\Delta z_{upper}^* = 0.0$. At the final stage of the process some molecules of the tip adhere to the lower plate and necking phenomena are observed. The initial shape of the tip is hardly seen in the final stage. It may be argued that the necking resulting in the molecular transfer is a mechanism of material transfer occurring with the breakage of adhesive junction. The marginal change in the normal force during the receding process is associated with the necking phenomenon.

During the pressing process the region in the

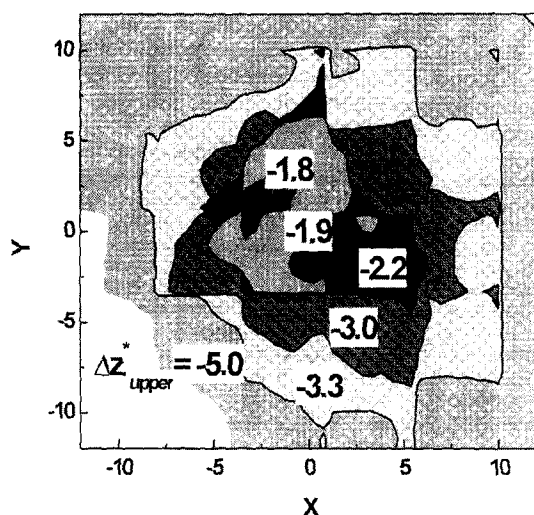


Fig. 2 Zones in the lower plate under the influence of the tip during the pressing process

lower plate interacting with the tip can be defined through estimating the interactive forces. Figure 2 shows the zones under the influence of the tip, which are the areas enclosed by the contour lines for each tip approach (Δz_{upper}^*). Although the shape of the tip is almost axisymmetric, the influenced zones are quite distorted due to the molecular dislocations during the pressing process.

So far the process is assumed isothermal, which is not realistic. For the isothermal process the temperature of the tip as well as those of the upper and lower plates are controlled to remain at $T^* = 0.248$. This implies that the potential energy increased by the pressing process has been changed into kinetic energy, that is absorbed by artificial cooler molecules promptly, that is, mathematically by the velocity scaling scheme (Haile, 1992). Since the temperatures of the tip molecules remain around $T^* = 0.248$, the tip remains to be solid-phase. If the velocity scaling scheme is not employed the increased potential energy changes into molecular kinetic energy, which implies increase of molecular temperatures. Since very high energy is required for this pressing process, this consumed energy increases the molecular internal energy, and thus some molecules may melt and evaporate. Figure 3(a) shows the snapshot of molecular distribution at the final stage of this case. The snapshot shows

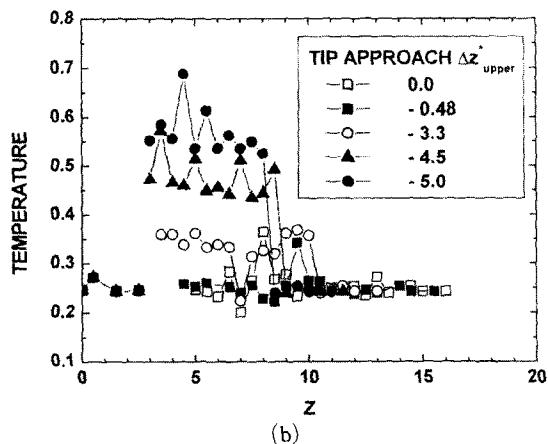
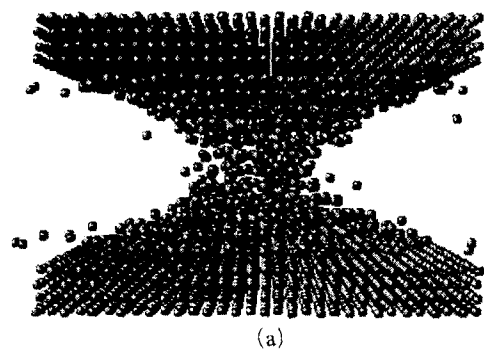


Fig. 3 (a) Snapshot of molecular distribution and (b) tip-temperature variation without velocity scaling for constant tip-temperature

some liberated molecules as well as the transferred molecules and the neck that are observed in the isothermal cases. Figure 3(b) shows the variation of tip temperature, averaged in the x - y plane, along the axis of symmetry at different tip locations during the approach period. Although the temperatures of the upper and lower plates are maintained at $T^*=0.248$ and there is a conduction heat transfer from the tip and the plates, the tip temperature increases very significantly beyond its melting temperature.

For a binary system the LJ potential can be modified (Diaz-Herrera et al., 1999) as

$$\Phi(r_{ij}) = 4\epsilon \left[\left(\frac{\sigma}{r_{ij}} \right)^{12} - \alpha \left(\frac{\sigma}{r_{ij}} \right)^6 \right] \quad (4)$$

where the parameter α controls the affinity between the tip/upper-plate molecules and the lower plate molecules, and ϵ and σ are the same for all interactions. For α less than unity the attractive force between the different molecules is weaker than that between the same-type molecules, and thus less interaction occurs. Figure 4 shows the molecular distribution at the final stage of the isothermal adhesion process when α is 0.5. Although the shape of the tip has been changed and smashed considerably, neither necking nor molecule transfer is observed.

Figure 5 shows the variation of the normal force imposed on the tip during adhesion processes. This irreversible phenomenon is known as adhesion hysteresis and has been observed experimentally (Chaudhury and Whitesides, 1991;

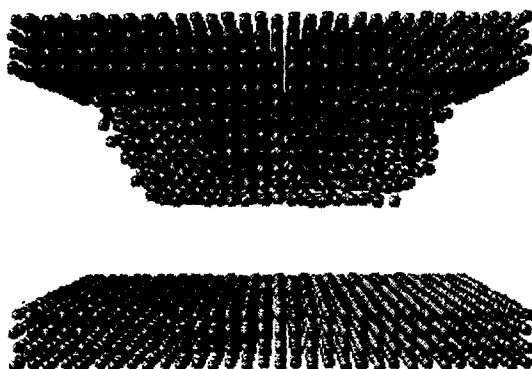
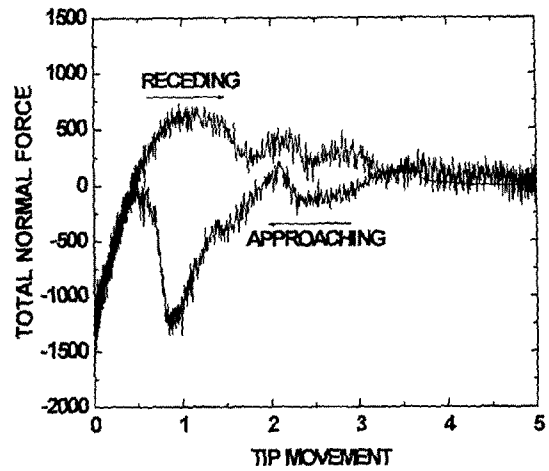
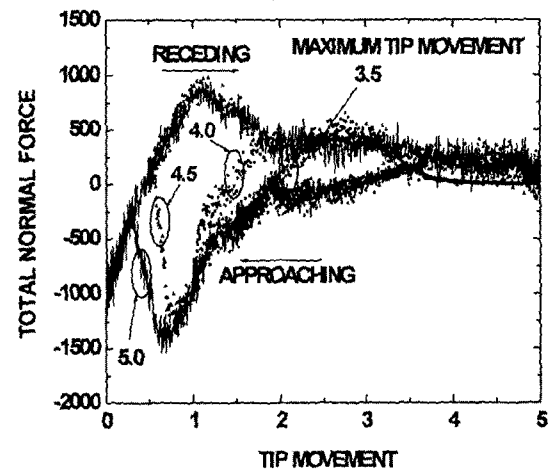


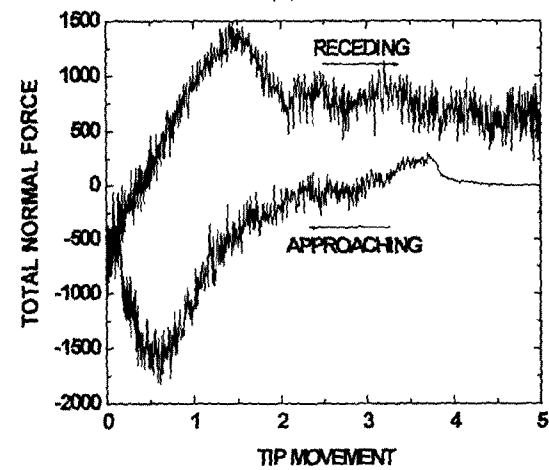
Fig. 4 Snapshot of molecular distribution for the affinity factor $\alpha=0.5$



(a)



(b)



(c)

Fig. 5 Hysteresis curves of normal forces for different tip sizes: (a) $R_{tip}^*=7.8$, (b) $R_{tip}^*=9.37$ (c) $R_{tip}^*=15.6$

Chen et al., 1991). Positive values imply attractive interaction, while negative ones do repulsive forces. In the beginning stage of a pressing process the tip approaches the lower plate and experiences relatively weak attraction. As the tip moves further down toward the lower plate, the interaction changes into repulsive one and there is a slight increase in the normal force, which is associated with the collapse of the first molecular layer of the tip. When the tip continues to move down, the repulsive force increases significantly and an abrupt decrease in the interaction occurs due to the collapse of the second layer of the tip. With the onset of the receding process the repulsive interaction turns into attraction monotonically and rapidly until the maximum attractive force is reached. As the tip moves upward further, the attractive forces tend to decrease, while the necking and molecular transfer phenomena occur. This hysteresis has been observed for different sizes of tips $R_{tip}^* = 7.8, 9.37, \text{ and } 15.6$, as shown in Figs. 5(a)-(c). Those hysteresis curves for different tip-sizes are qualitatively identical although the increase in the tip size enhances the magnitudes of the maximum attractive and repulsive forces and thus the energy dissipation due to adhesion hysteresis. The hysteresis curves for various maximum tip approaches are shown in Fig. 5 (b). The hysteresis curves for different maximum tip approaches are almost identical except the period during which the monotonic and rapid transition from repulsion to attraction occurs with the onset of recession.

Figure 6 shows the force variations in the cases of isothermal processes of affinity factors, α of 1.0 and 0.5 and the process without tip-temperature control. Allowing the change in the tip temperature reduces the magnitudes of both the repulsive force at the final stage of the pressing process and the attractive force during recession since melting of some molecules with the temperature rise is considered in the simulation. With a smaller affinity factor the interaction during recession becomes weak, as expected from Fig. 4, while the interaction during approach is marginally influenced.

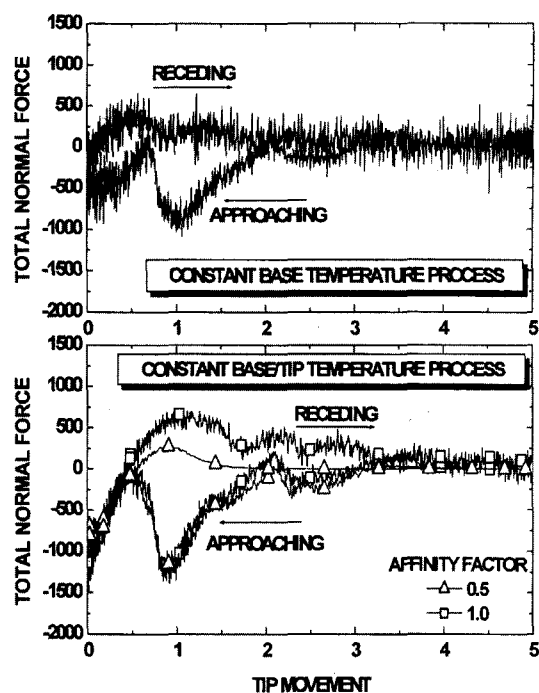


Fig. 6 Dependence of hysteresis curve on affinity factor and tip temperature

4. Conclusions

Using molecular dynamics technique the adhesion process has been simulated for the Lennard-Jones molecules. Although the LJ model is one of the simplest models and considers only the Pauli repulsion and van der Waals attraction, the model simulates the physical behavior observed in experiments.

In the approaching period the attractive interaction turns into the repulsive one with the onset of physical contact. With further approach the repulsive force becomes stronger with the fluctuation of interaction forces associated with the collapse of molecular layers. In the receding period the interaction changes from repulsion into attraction monotonically and rapidly and then vanishes gradually. These characteristics of hysteresis curve are observed in all the simulations conducted with different-size tips, with different maximum tip approaches, with different tip-temperature control schemes, and with different tip-surface affinity factors. The change in the

maximum tip approach influences only the rapid transition from repulsion to attraction occurring at the beginning of recession period in the hysteresis curve.

Some molecules of the tip are transferred to the surface during the recession. The tip material transfer is also observed in the case that the temperature variation is allowed. When the tip material differs from the mating plate material, the material transfer does not occur although the tip is deformed plastically.

Acknowledgment

The authors gratefully acknowledge financial support from University Research Program conducted by Ministry of Information & Communication in Korea. In addition, S. H. Park has been partially supported for this research by Micro Thermal System Research Center.

References

- Allen, M. P. and Tildesley, D. L., 1987, *Computer Simulation of Liquids*, Oxford University Press, New York.
- Chaudhury, M. K. and Whitesides, G. M., 1991, "Direct Measurement of Interfacial Interactions Between Semispherical Lenses and Flat sheets of Poly(Dimethylsiloxane) and Their Chemical Derivatives," *Langmuir*, Vol. 7, pp. 1013~1025.
- Chen, Y. L., Helm, C. and Israelachvili, J. N., 1991, "Molecular Mechanisms Associated with Adhesion and Contact Angle Hysteresis of Monolayer Surfaces," *J. Phys. Chem.*, Vol. 95, pp. 10736~10747.
- Cho, S. -S. and Park, S. H., 2002, "Finite Element Modeling of Hemispherical Asperity Adhesively-Contacting the Plane Surface of Semi-Infinite Rigid Body," *Journal of KSME A (submitted)*.
- Christopher, D., Smith, R. and Richter, A., 2001, "Nanoindentation of Carbon Materials," *Nuclear Instruments and Methods in Physics Research B*, Vol. 180, pp. 117~124.
- Derjaguin, B. V., Muller, V. M. and Toporov, Yu. P., 1975, "Effect of Contact Deformations on the Adhesion of Particles," *Journal of Colloid and Interface Science*, Vol. 53, No. 2, pp. 314~326.
- Diaz-Herrera, E., Alejandre, J., Ramirez-Santiago, G. and Forstmann, F., 1999, "Interfacial Tension Behavior of Binary and Ternary Mixtures of Partially Miscible Lennard-Jones Fluids: a Molecular Dynamics Simulation," *J. Chem. Phys.*, Vol. 110, pp. 8084~8089.
- Haile, J. M., 1992, *Molecular Dynamics Simulation*, John Wiley & Sons, pp. 260~267.
- Johnson, K. L., Kendall, K., and Roberts, A. D., 1971, "Surface Energy and the Contact of Elastic Solids," *Proc. R. Soc. Lond.*, Vol. 324, pp. 301~313.
- Komanduri, R., Chandrasekaran, N. and Raff, L. M., "MD Simulation of Indentation and Scratching of Single Crystal Aluminum," *Wear*, Vol. 240, pp. 113~143.
- Landman, U., 1998, "On Nanotribological Interactions: Hard and Soft Interfacial Junctions," *Solid State Communications*, Vol. 107, No. 11, pp. 693~708.
- Park, S. H., Lee, J. S., Choi, Y. K. and Kim, H. J., 2002, "Vibration Induced Crystallization of Amorphous Materials: Molecular Dynamics Study," *ICHMT Conference*, Antalya, Turkey.
- Rabinowicz, E., 1965, *Friction and Wear of Materials*, John Wiley & Sons, New York, pp. 52~108.
- Rafii-Tabar, H., 2000, "Modelling the Nano-Scale Phenomena in Condensed Matter Physics Via Computer-Based Numerical Simulations," *Physics Reports*, Vol. 325, pp. 239~310.
- Richter, A., Ries, R., Smith, R., Henkel, M. and Wolf, B., 2000, "Nanoindentation of Diamond, Graphite and Fullerene Films," *Diamond and Related Materials*, Vol. 9, pp. 170~184.
- Straffelini, G., 2001, "A Simplified Approach to the Adhesive Theory of Friction," *Wear*, Vol. 249, pp. 79~85.
- Swope, W. C., Anderson, H. C., Berens, P. H. and Wilson, K. R., 1982, "A Computer Simulation Method for the Calculation of Equilibrium Constants for the Formation of Physical Clusters of Molecules: Application to Small Water Clusters," *J. Chem. Phys.*, Vol. 76, pp. 637~649.

Weng, J. G., Park, S. H, Lukes, J. R. and Tien, C. L., 2000, "Molecular Dynamics Investigation of Thickness Effect on Liquid Films," *J. Chem. Phys.*, Vol. 113, pp. 5917~5923.

Zhang, L. and Tanaka, H., 1997, "Towards a Deeper Understanding of Wear and Friction on the Atomic Scale-A Molecular Dynamics Analy-

sis," *Wear*, Vol. 211, pp. 44~53.

Zhang, L. and Tanaka, H., 1998, "Atomic Scale Deformation in Silicon Monocrystals Induced by Two-Body and Three-Body Contact Sliding," *Tribology International*, Vol. 31, No. 8, pp. 425~433.